

PAPER • OPEN ACCESS

## Influence of severe plastic deformation on the structure and mechanical properties of eutectic Al-Zn-Mg-Fe-Ni alloy

To cite this article: I G Brodova *et al* 2019 *IOP Conf. Ser.: Mater. Sci. Eng.* **672** 012022

View the [article online](#) for updates and enhancements.

**INTERNATIONAL OPEN ACCESS WEEK**  
OCTOBER 19-26, 2020

**ALL ECS ARTICLES. ALL FREE. ALL WEEK.**  
[www.ecsdl.org](http://www.ecsdl.org)

**NOW  
AVAILABLE**

# Influence of severe plastic deformation on the structure and mechanical properties of eutectic Al-Zn-Mg-Fe-Ni alloy

I G Brodova<sup>1,2</sup>, A N Petrova<sup>1</sup> and T K Akopyan<sup>3</sup>

<sup>1</sup> M.N. Mikheev Institute of Metal Physics of Ural Branch of Russian Academy of Sciences, 620108, 18 S. Kovalevskoy Street, Ekaterinburg, Russia

<sup>2</sup> Ural Federal University named after the first President of Russia B. N. Yeltsin, 620002, 19 Mira Street, Ekaterinburg, Russia

<sup>3</sup> National University of Science and Technology MISiS, 119049, 4 Leninsky av., Moscow, Russia

E-mail: brodova@imp.uran.ru

**Abstract.** The structure and phase evolution of the new eutectic high strength aluminium alloy Nikalin were investigated under high pressure torsion (HPT) by several numbers of the revolution of the anvil. The chemical composition of the investigated Nikalin alloy was as follows: Al (base)–7.22Zn–2.95 Mg–0.52 Fe–0.57 Ni–0.2 Zr. (wt.%). The initial material was a coarse grained cast ingot after homogenization. It was established that the HPT process resulted in the deformation dissolution of the nanosized T-phase precipitates and the formation of a supersaturated aluminum solid solution simultaneously with the strong refinement of the structure to the grain-subgrain size of 130-150 nm. Due to that, the yield stress of the HPT alloy increased by a factor of 1.5, the ultimate tensile strength increased by a factor of 1.4, while preserving good ductility of 6-7%. The observed effect of the additional supersaturated solution upon HPT relative to the homogenized state appeared upon post-deformation annealing at 140 °C. An increase in the microhardness of the HPT alloy due to the MgZn<sub>2</sub> phase precipitation was observed at 0.5- hours of annealing.

## 1. Introduction

The Nikalins is the name of a new class of eutectic aluminum based alloys. The structure and properties of the castings, rolled sheets and radial-shear rolling rods of the high-strength alloy (Al-7Zn-3Mg-Fe-Ni) were recently investigated [1-3]. The results showed the potential of the thermo-deformation treatment for producing high strength semi-finished products of good quality.

It is well known that high pressure torsion (HPT) is an effective technique for improving the structure of aluminum-based materials and their mechanical properties [4-6]. An analysis of the published papers has shown that the structure and deformation behavior of eutectic alloys produced by the HPT process have not been adequately studied, and have not been studied earlier for alloys of the Nikalin type.

The purpose of the present work is to investigate the peculiarities of the structural-phase transformations during HPT, to determine the hardening mechanisms during deformation and post deformation annealing, and to determine the mechanical properties of an alloy of the Al-Zn-Mg-Fe-Ni system.



## 2. Experimental

The chemical composition of the investigated Nikalin alloy was as follows: Al (base)–7.22Zn–2.95 Mg–0.52 Fe–0.57 Ni–0.2 Zr. (wt. %). The initial material was a cast ingot after two-stage homogenizing annealing at 450 °C and at 540 °C for 3 hours at each stage. The choosing of the homogenization regime is described in [2]. The material had an initial static yield stress  $\sigma_y = 220$  MPa, a tensile strength  $\sigma_u = 350$  MPa, and a microhardness  $H_v = 1400$  MPa.

Cross-sectional discs with a thickness of 1.2 mm were cut from a billet with a diameter of 20 mm. The discs were processed by HPT at room temperature. The accumulated true strain varied between  $\epsilon = 6.0, 6.7$ , and  $7.1$ , corresponding to the number of revolutions of the anvil  $n = 5, 10$  and  $15$ . The accumulated true strain was calculated for the half radius of the HPT samples, considering pre-stressing to a thickness of 1 mm. The produced samples were used for structural investigations, static tensile tests and post deformation annealing.

Structural investigations were performed by means of a Tecnai G2 30 Twin transmission electron microscope (TEM) and a Quanta-200 scanning electron microscope (SEM). X-ray diffraction (XRD) analysis was carried out using an Empyrean (PANalytical) diffractometer at room temperature and  $\text{CuK}\alpha$  radiation. Based on the X-ray diffraction data, the lattice parameter of the aluminium matrix and the mean-square microstrain of the crystal lattice were calculated. Hardness  $H_v$  was measured using a PMT-3 device at a load of 0.2 N (the error did not exceed 10%).

For static mechanical tests, two tensile specimens with a gauge length of 5.7 mm, a width of 2.0 mm, and a thickness of 1 mm were machined from the HPT disc using electrical discharge machining. Microspecimens were pulled to failure using a Shimadzu AGX-50 Plus universal testing machine. Tensile tests were conducted at room temperature and at a strain rate of  $\dot{\epsilon} = 2 \times 10^{-3} \text{ s}^{-1}$ . Structural investigations and hardness measurements were conducted at half the radius of the HPT samples. The shape of the tensile microsamples and the scheme of a cut-off appear to provide the measurements of static mechanical properties at half the radius area of the HPT discs.

Tensile tests of the homogenized cast alloy were conducted on standard cylindrical specimens at a strain rate  $\dot{\epsilon} = 2.5 \times 10^{-3} \text{ s}^{-1}$  by means of a Zwick Z250 testing machine according to ASTM E 8/E 8M-08.

## 3. Results

### 3.1. Mechanical properties

The obtained experimental  $\sigma$ - $\epsilon$  diagrams of HPT alloys are shown in a figure 1a. Figures 1b and 1c demonstrate the yield stress  $\sigma_y$  and microhardness depending on the number of revolutions  $n$ . It is shown that the yield stress value changes consistently with an increase in the accumulated strain as well as microhardness. The highest values of  $\sigma_y = 521$  MPa and  $H_v = 2900$  MPa correspond to the samples after HPT,  $n = 10$ . With increasing  $n$  up to 15, these mechanical characteristics decrease by 100 and 340 MPa. The tensile strength of HPT Nikalin is higher by a factor of 1.4 compared to that of the initial homogenized alloy. The plasticity of HPT samples is  $\delta = 6$ -7% at various  $n$ .

### 3.2. Structure and phase composition

To explain the observed regularities of the mechanical behavior of Nikalin and the hardening mechanisms during HPT, the evolution of the structure and phase composition depending on the accumulated strain has been studied.

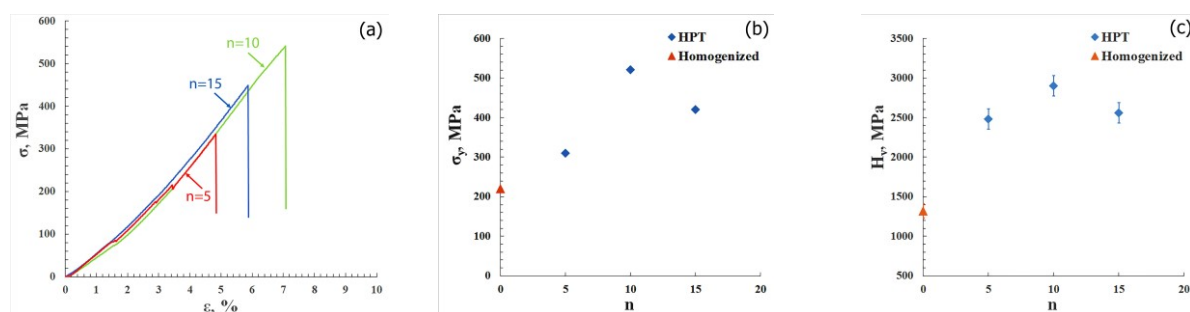


**Figure 1.** Mechanical properties of the HPT alloy: a - stress-strain diagrams, b - yield stress and c - microhardness changes depending on the number of revolutions.

The phase composition of the alloy after homogenization is represented by the Al (Zn, Mg) solid solution, the eutectic (Al + Al<sub>9</sub>FeNi), and the T phase - Al<sub>2</sub>Zn<sub>3</sub>Mg<sub>3</sub>.

The quantitative analysis of the structure has shown that the average grain size was 380 μm (figure 2a). The eutectic Al<sub>9</sub>FeNi aluminides are arranged in groups along the grain boundaries. The thickness of the eutectic layer is 2 μm (figure 2b). The secondary T phase precipitated during cooling after homogenization. The T phase particles with a size of 15-20 nm are shown up predominantly within the grains (figure 2c).

The evolution of each structural component under deformation was investigated considering the complex phase composition of the homogenized alloy. According to SEM data, the morphology and the size of the Al<sub>9</sub>FeNi aluminides slightly change upon HPT compared to the initial state. Because of the almost zero solubility of iron and nickel in the Al solid solution, the content of the eutectic phase retained unchanged before and after HPT. The eutectic Al<sub>9</sub>FeNi aluminides are arranged in groups after HPT (n=5, 10). An increase in strain leads to a uniform distribution of the particles (n=15).

The results of structural investigations of the alloy after HPT treatment (n=5 and n=15) are shown in figure 3. After HPT (n=5), a shear band structure was formed (figure 3a). The TEM image represents a slightly misoriented fine subgrained structure within the bands (figure 3b). An increase in *n* leads to the development of crystals fragmentation, rotations modes results in the formation of HABs and their predominance (figure 3d). An augmentation of point reflections on the circle type MD pattern at n=15 indicates an increase in the fraction of HABs (figure 3d). One can see deformed grains-subgrains with a strong deformation contrast as well as small (20-30 nm) defect-free grains that testify the onset of dynamic recrystallization (figure 3d). Thus, the mixed structure of deformed and recrystallized crystallites was formed after HPT, n=15.

The grain-subgrain size distributions are constructed depending on the accumulative strain. A slight decrease in the size of the Al-matrix fragments from 155±75 nm to 130±75 nm was established with an increase in *n*. Thus, the HPT treatment results in significant grain refinement as compared with the grain size of the initial alloy. An increase in the accumulated strain leads to a transition from a fragmented structure with a developed LABs network to a mixed submicrocrystalline structure with a predominance of HABs.

Figure 4 shows the segments of the x-rays patterns for the initial homogenized alloy and for the alloy after HPT. For these patterns, all reflection lines refer to the Al solid solution and to the Al<sub>9</sub>FeNi aluminides. An increase in the mean-square microstrain from 0.13% up to 0.19% was observed with an increase in the accumulated strain *n*. The lattice parameter was *a*=0.4059 nm for the homogenized alloy and did not change upon HPT (*a*=0.4058-0.4060 nm, Δ*a* = 0.0001-0.0002 nm). The constant lattice parameter values cannot indicate the absence of diffusion of the atoms of the dissolved elements into the solid solution, because Mg atoms increase the aluminum lattice parameter, and Zn atoms decrease it.

According to the TEM data, the nanosized T-phase particles were presented in the structure of HPT alloys (figure 3c). The absence of reflections from this phase on the x-rays patterns of the deformed samples is due to its small volume fraction. The volume fraction of the T phase particles decreases with increasing accumulated strain and only single particles of the T phase are precipitated within the grain-subgrains of samples after the HPT, *n* = 10 and *n* = 15. Thus, with an increase in the accumulated strain, the

deformation dissolution of aluminides and the formation of a supersaturated Al solid solution occur, but given the data of the works [6,7], we can assume that Zn and Mg atoms from the disappeared aluminide precipitates were used for the formation of adsorption layers in GBs. To confirm these phenomena, additional studies of structural phase transformations in HPT Nikalin are planned using STEM and Atom probe tomography.

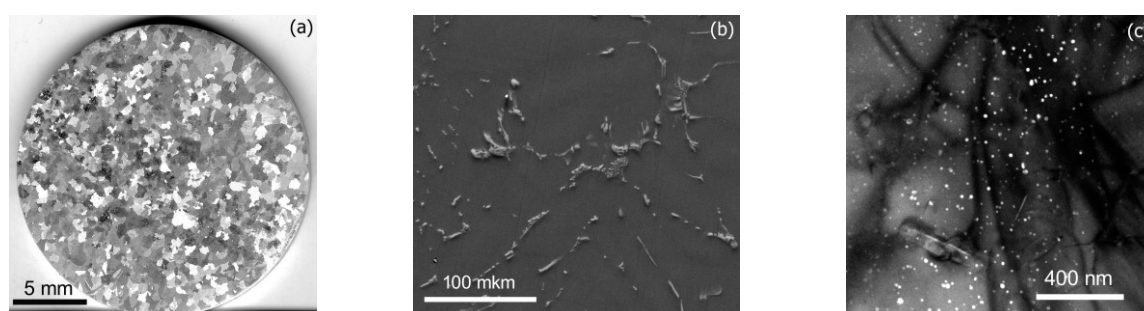


**Figure 2.** Structure of the homogenized alloy: a - grains, b - SEM image of  $\text{Al}_9\text{FeNi}$  particles, c - DF TEM image of the  $\text{Al}_2\text{Mg}_3\text{Zn}_3$  hardening phase.

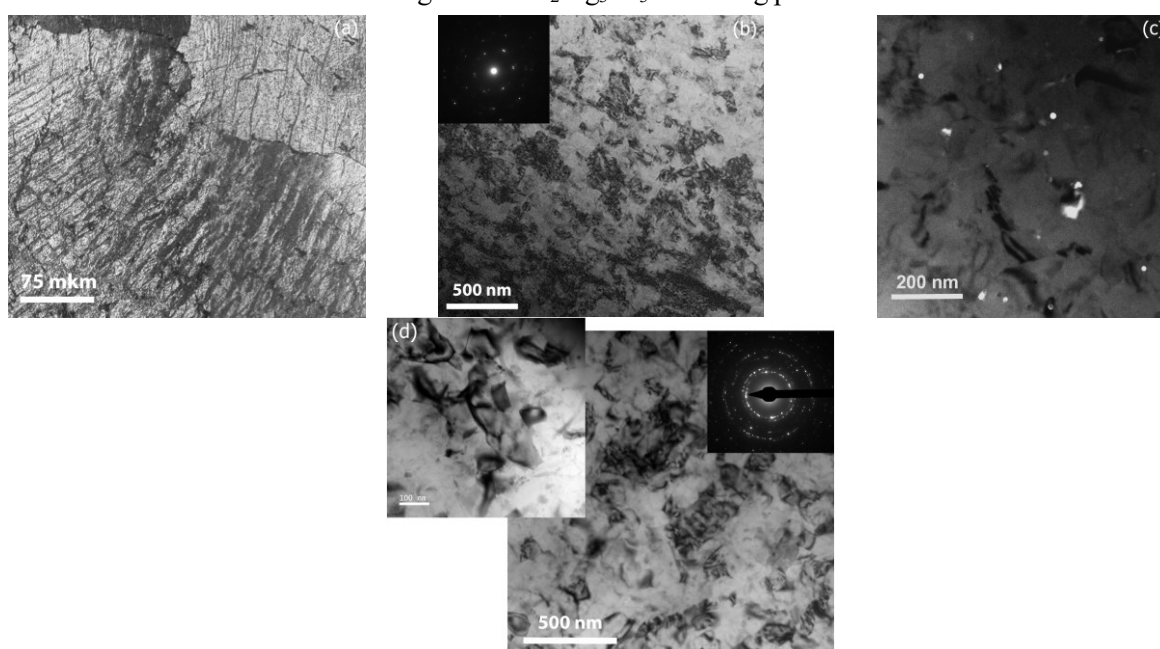


**Figure 3.** Structure of the HPT alloy: a - band structure after  $n=5$ , b - submicrocrystalline structure after  $n=5$ , c -  $\text{Al}_2\text{Mg}_3\text{Zn}_3$  phase particles (DF TEM), d - submicrocrystalline structure after  $n=15$ .

The observed effect of an additional supersaturation solution relative to the homogenized state appears upon post-deformation annealing of HPT samples at 140 °C for 6 hours. X-rays analysis shows that this treatment results in the reduction of the concentration of defects and in decreasing lattice parameter to  $a=0.4046$  nm. The mean-square microstrain after annealing is reduced to 0.12%-0.08%. On the X-rays patterns of the aged HPT samples, the additional reflection lines were determined. These lines correspond to the stable  $\text{MgZn}_2$  phase (figure 4). The effect of the supersaturated solid solution decomposition leads to non-monotonic microhardness-time dependences. In spite of the general tendency toward the microhardness decrease due to the recovery, an increase in the microhardness at short exposures of about 0.5 and 1 hours was observed. The effect of dispersion hardening in samples with greater accumulated strain appears at shorter annealing times.

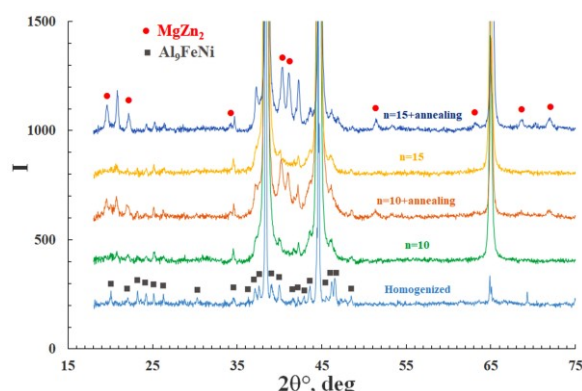


**Figure 4.** X-rays diffraction patterns for the homogenized, HPT alloy and HPT alloy after annealing.

After 6 hours of annealing, the HPT samples have high hardness of 1700–1800 MPa. Thus, the decrease in hardening is compensated by the preservation of the grain boundary hardening according to the Hall-Patch law and the dispersion hardening with the formation of a stable nano-sized  $\text{MgZn}_2$  phase. A similar increase in the hardness of the quenched alloy occurs at the same temperature of artificial aging only after a long exposure for more than 3 hours [7]. Thus, the formation of the submicrocrystalline structure changes the precipitation kinetics and the type of precipitates of the hardening phases. The  $\text{MgZn}_2$  phase particles precipitated from the supersaturated aluminum solid solution after HPT treatment. Aging of the quenched alloy leads to the formation of T-phase precipitates.

#### 4. Conclusions

The HPT experiment showed that severe plastic deformation had a strong influence on the structure and properties of Nikalin. It was established that a submicrocrystalline deformed structure with an average size of grain-subgrains of 130-150 nm was formed after HPT. The growth of the stress state of the HPT alloy ( $n=15$ ) activated the process of dynamic recrystallization, and a mixed structure was formed consisting of deformed fragments and recrystallized grains.

It was established that in the HPT process, the accumulation of structural defects (vacancies and dislocations), the deformation dissolution of nanosized T-phase precipitates, and the formation of a supersaturated aluminum solid solution occur simultaneously with the refinement of the structure.

The alloy with the submicrocrystalline structure had high mechanical properties as compared with the initial homogenized state. The yield stress of the HPT samples increased by a factor of 1.5, the ultimate tensile strength increased by a factor of 1.4, while preserving the same ductility of 6-7%.

X-ray diffraction and microhardness measurements were used to establish structural and phase transformations with post-deformation annealing at 140 °C from 0.25 to 6 hours. It was found that the preliminary HPT deformation significantly accelerated the decomposition of the supersaturated aluminum solid solution. The effect of dispersion hardening is observed already after 0.5-1 hours of annealing of the submicrocrystalline alloy at 140 °C. In addition, the formation of the submicrocrystalline structure changes the precipitation kinetics and type of precipitates of the hardening phases. It was determined that 6-hour annealing at 140 °C did not cause degradation of the submicrocrystalline structure and HPT Nikalin retained high strength.

#### Acknowledgments

The research was carried out within the state assignment of the Ministry of Science and Higher Education of the Russian Federation (theme “Structura”, № AAAA-A18-118020190116-6) supported in part by RFBR (project № 18-03-00102). The electron microscopy investigations were performed at the Center of Collaborative Access “Testing Center of Nanotechnologies and Advanced Materials” of the M.N. Mikheev Institute of Metal Physics of Ural Branch of Russian Academy of Sciences.

**References**

- [1] Belov N, Akopyan T and Naumova E 2017 *Mater. Sci. Technol.* **33** 656
- [2] Shurkin P K, Belov N A, Akopyan T K, Aleshchenko A S, Avxentieva N N and Alabin A N 2017 *Phys. Met. Metallogr.* **118** 896
- [3] Shurkin P K, Akopyan T K, Galkin S P and Aleshchenko A S 2019 *Metal Science and Heat Treatment* **60** 764
- [4] Sabirov I, Murashkin M Y and Valiev R Z 2013 *Mater. Sci. Eng. A* **560** 1
- [5] Zhang Y D, Jin S B, Trimby P, Liao X Z, Murashkin M Y, Valiev R Z and Sha G 2019 *Mater. Sci. Eng. A* **752** 223
- [6] Sauvage X, Murashkin M Yu, Straumal B B, Bobruk E V, Valiev R Z 2015 *Adv. Eng. Mater.* **17** 1821
- [7] Nguyen Q C, Csanádi T, Györi T, Valiev R Z, Straumal B B, Kawasaki M, Langdon T G 2012 *Mater. Sci. Eng. A* **543** 117